J Mater Sci (2011) 46:2273–2280
DOI 10.1007/s10853-010-5067-2

Crystal-growth inhibition of solid porphyrin micro-crystals by G4 PAMAM dendrimer

Walid M. Hikal · H. James Harmon

Received: 25 August 2010 / Accepted: 9 November 2010 / Published online: 24 November 2010

Abstract We report on the effect of G4 PAMAM dendrimer on the formation of a previously reported solid porphyrin micro-crystals formed by two oppositely charged porphyrins [meso-tetra(*N*-methy-4-pyridyl)porphyrin tetratosylate (TMPyP) and zinc-tetrakis(4-sulphonatophenyl)-porphyrin (Zn-TPPS)], by self-assembly at room temperature without acidification. The crystals were characterized by UV–visible spectroscopy, fluorescence spectroscopy, optical microscopy, and powder X-ray diffraction techniques. The addition of the G4 PAMAM dendrimer to the starting solution of the monomer porphyrins alters the size and morphology of the crystals as well as their absorbance and fluorescence spectra. However, the dendrimer is not incorporated in the structure.

Introduction

Porphyrins possess particular photo-physical and photochemical properties that depend on the substituents attached to the tetrapyrrolic ring as well as the metal linked to the nitrogen atoms in the core of the porphyrin ring [1, 2]. Porphyrins play a principle role in many biochemical reactions including photosynthesis, drug detoxification, oxidation, and electron transfer [3–7]. Molecular self-assembly is a stratagem for the fabrication of many new materials involving the spontaneous aggregation of small molecular entities into specific structures in liquid or solid environments by a variety of cooperative and directional intermolecular interactions. Molecular self-assembly orders the molecular components in space to form supramolecular entities with predefined dimensionality and connectivity [8]. Self-assembled, self-organized, and covalently bound porphyrin arrays are attractive building blocks for the modular construction of tailored field-responsive materials and provide a versatile tool for potential applications in the design of sensors, catalysts, electronic and photonic devices, molecular sieves, and solar energy conversion devices [9–14].

Recently, we have reported on the formation of highly stable solid porphyrin micro-crystals using water-soluble porphyrins [meso-tetra(*N*-methy-4-pyridyl)porphyrin tetratosylate (TMPyP) and zinc-tetrakis(4-sulfonatophenyl)porphyrin (Zn-TPPS)], at room temperature without pH control [15]. The crystals have been shown to be an efficient photo-catalyst for 2,4,6-trinitrotoluene (TNT) destruction. However, the degradation process takes place only on the surface of the crystals (binding sites between crystals and TNT). In order to decrease the amount of the sacrificed porphyrin molecules in the core of the micro-crystals, since smaller objects will have larger surface area, and to further enhance the functional ability of these crystals as a photo-catalyst, we report on the effect of polyamidoamine (PAMAM) generation 4 (G4) dendrimer on the shape, size, and optical properties of the previously reported porphyrin micro-crystals when formed in its presence. The crystalline structure was investigated and characterized by light microscopy, UV–visible spectroscopy, fluorescence spectroscopy, and powder X-ray diffraction to determine the role of the dendrimer in shaping these crystals.

W. M. Hikal (✉) · H. J. Harmon
Department of Physics, Oklahoma State University, Stillwater, OK 74078, USA
e-mail: wmhikal@gmail.com

Experimental procedure

Materials

Meso-tetra(*N*-methy-4-pyridyl)porphyrin tetratosylate (TMPyP) and zinc-tetrakis(4-sulfonatophenyl)porphyrin (Zn-TPPS), shown in Fig. 1, were obtained from Frontier Scientific (Logan, UT) and used without further purification. Stock porphyrin solutions (1 mM) were prepared in 18 mΩ de-ionized water, stored refrigerated, and used within 2 weeks of preparation. PAMAM dendrimer generation 4 (G4) in methanol was obtained from Sigma-Aldrich, Inc. (St. Louis, MO) and kept refrigerated until use. PAMAM dendrimer was dried using nitrogen gas before mixing with porphyrins in de-ionized water.

Spectroscopic techniques

Absorbance spectra of the porphyrin monomers in pH 7.0 phosphate buffer and the absorbance spectra of the immobilized porphyrin crystals were collected using a Cary 5E UV–visible spectrophotometer at 0.5 nm resolution using de-ionized water or a microscope slide as a reference depending on the sample being measured.

Fluorescence measurements were made with a SPEX FluoroMax-3 (Jobin–Yvon, Inc. Edison, NJ). Very dilute solutions (1 μM) were used to avoid spectral distortions due the inner filter effect and emission re-absorption. Before measuring fluorescence spectra of TMPyP, the cuvettes were cleaned with nitric acid since TMPyP has a marked tendency to adhere on the cuvette walls.

Results

UV–visible study of porphyrins interaction with G4 PAMAM dendrimer

The absorbance spectrum of zinc-tetrakis(4-sulfonatophenyl)porphyrin (Zn-TPPS) at pH 7.0 in the absence of G4 PAMAM dendrimer at room temperature exhibits an absorbance peak in the Soret region at 421 nm and two

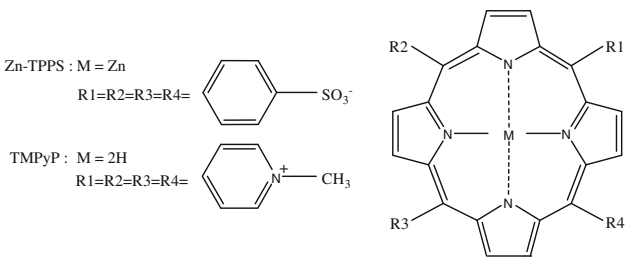

Fig. 1 Chemical structures of porphyrins used in making the porphyrin crystals

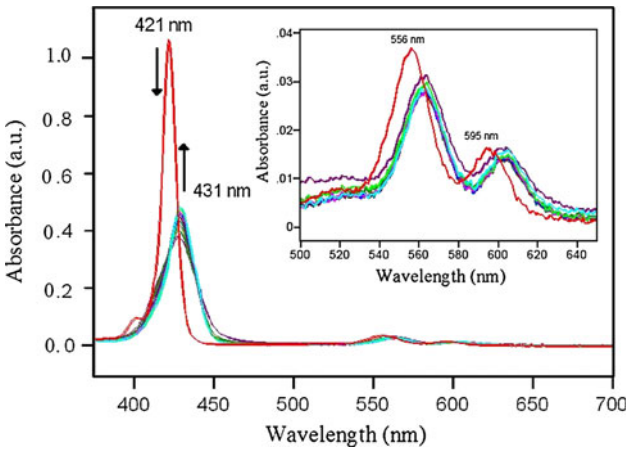

Fig. 2 Absorbance spectra of 1.6 μM zinc-tetrakis(4-sulfonatophenyl)porphyrin (Zn-TPPS) in the absence (*top spectrum*) and presence of G4 PAMAM dendrimer (0.43, 0.57, 1.14, 1.72, 2.29, 2.86, 5.72, 8.58, 11.44, and 14.3 μM, respectively) at pH 7.0 and room temperature. *Arrows* show the spectral changes upon increasing the G4 PAMAM dendrimer concentration

Q-bands at 556 and 597 nm. As shown in Fig. 2, upon the addition of G4 PAMAM dendrimer (0.43, 0.57, 0.72, 0.86, 1.14, 1.43, 1.72, 2.29, 2.86, and 4.29 μM, respectively) to 1.67 μM Zn-TPPS, both the Soret band and the Q-bands of Zn-TPPS shift to longer wavelengths. The new Soret peak is located at 431 nm and the new Q-bands are located at 565 and 606 nm as determined using the second derivatives of the absorbance spectra of Zn-TPPS in the presence of G4 PAMAM dendrimer. The decrease in the Soret band of Zn-TPPS indicates a decrease in the concentration of the uncomplexed Zn-TPPS in the solution. The appearance of a different Soret peak and Q-bands are results of the formation of a new dendrimer-porphyrin complex. Using Grams/32, the spectra of Zn-TPPS in the presence of G4 PAMAM dendrimer were deconvoluted into two peaks at 421 nm (Soret peak of unbound Zn-TPPS) and 431 nm (Soret peak of Zn-TPPS-dendrimer complex) with correlation (r^2) of 0.99946. The areas under the two peaks at different G4 PAMAM concentrations were calculated using Grams/32 and normalized to unity to determine the individual contribution of each peak to the observed Soret band. As shown in Fig. 3, a plot of the normalized areas under the two peaks versus the concentration of G4 PAMAM dendrimer added to the solution results in two curves showing the decrease in the 421 nm peak and the increase in the 431 nm peak upon the addition of G4 PAMAM dendrimer. The two curves intercept at G4 PAMAM dendrimer concentration of 1.73 μM. Since 1.67 μM Zn-TPPS was used, data suggest a one-to-one stoichiometry between Zn-TPPS and G4 PAMAM dendrimer.

The absorbance spectrum of meso-tetra(*N*-methyl-4-pyridyl)porphyrin (TMPyP) exhibits an absorbance peak at the Soret region at 422 nm, and four Q-bands at 519, 553,

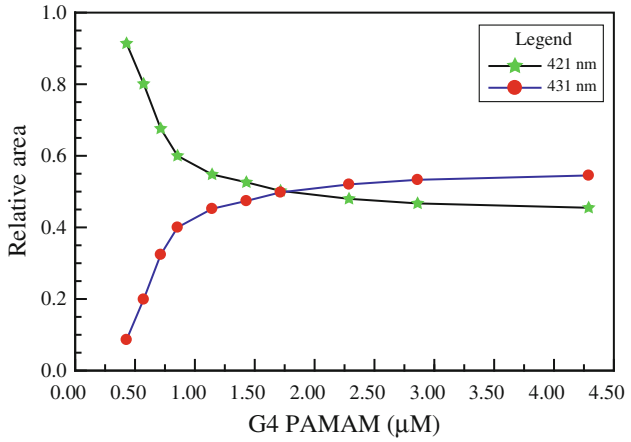

Fig. 3 A plot of the normalized areas under the deconvoluted spectra of 1.67 μM Zn-TPPS upon the addition of G4 PAMAM dendrimer (0.43, 0.57, 0.72, 0.86, 1.14, 1.4, 1.72, 2.29, 2.86, and 4.29 μM, respectively)

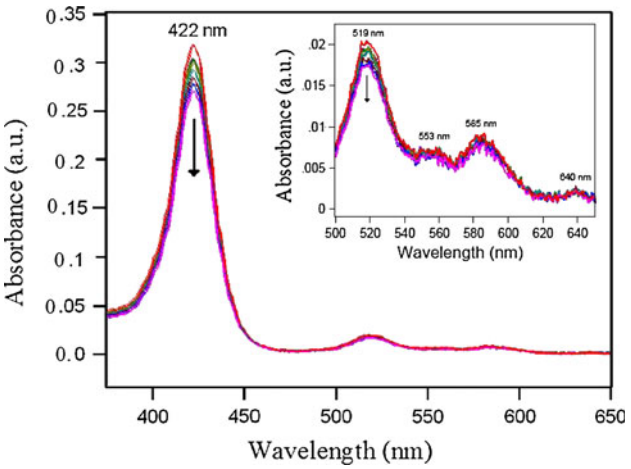

Fig. 4 Absorbance spectra of 1.6 μM meso-tetra(*N*-methyl-4-pyridyl)porphyrin (TMPyP) in the absence (*top spectrum*) and presence of G4 PAMAM dendrimer (0.572, 1.144, 2.86, 5.72, 8.58, 11.44, and 14.3 μM, respectively) at pH 7.0 and room temperature. *Arrows* show the absorbance decrease upon increasing the G4 PAMAM dendrimer concentration

585, and 640 nm. As shown in Fig. 4, upon the addition of G4 PAMAM dendrimer (0.572, 1.144, 2.86, 5.72, 8.58, 11.44, and 14.3 μM, respectively), the intensities of the absorbance peaks decrease, but no shift in the absorbance wavelengths is observed. The absence of any new absorbance peaks and isosbestic points indicate that G4 PAMAM dendrimer is not able to complex with TMPyP. This is expected since the two molecules are positively charged at pH 7.0. The decrease in the absorbance peaks is a result of the solution dilution as has been confirmed by comparison between the experimental data and the calculated absorbance using the extinction coefficient of TMPyP (2.066×10^5 M^{-1} cm^{-1}).

Formation of porphyrin micro-crystals

Porphyrin crystals were made by mixing 1:1 M ratios of solutions of zinc-tetrakis(4-sulfonatophenyl)porphyrin (Zn-TPPS) and meso-tetra(*N*-methyl-4-pyridyl)porphyrin (TMPyP) in 18 MΩ de-ionized water at room temperature in the presence of G4 PAMAM dendrimer. Mixing ratios of porphyrins that are different than unity result in excess porphyrin solution that is not incorporated in the crystals. Different porphyrin/dendrimer ratios have been used in making the porphyrin crystals. The pH of the solution was measured during the formation of the crystals and determined to be between 8.5 and 9.7 (due to the basic nature of the amino groups of the dendrimer). The aqueous mixture of the two oppositely charged porphyrins with G4 PAMAM dendrimer was kept undisturbed in the dark at room temperature for 24 h. However, the solid porphyrin crystals form immediately after mixing the two porphyrin monomers with the G4 PAMAM dendrimer.

The solid crystals were filtered and washed three times with de-ionized water, 95% ethanol, and pH 7.0 sodium phosphate (NaPi) buffer to remove any porphyrin excess.

As we have previously reported [15], in the absence of the dendrimer at 0.5 mM porphyrin concentration, the crystal dimensions are 30–40 μm × 10–25 μm × 4–6 μm. The concentration of porphyrins used in this work is also 0.5 mM. At porphyrin/dendrimer ratios = 1, the crystals have a length that ranges from 8 to 10 μm, a width between 6 and 8 μm, and a thickness between 2 and 4 μm as shown in Fig. 5a, and have a "X-like" shape when viewed while floating in solution as seen in Fig. 5b. At porphyrin/dendrimer concentration ratios <0.2, the crystals length ranges from 15 to 20 μm with width between 6 and 8 μm and thickness between 2 and 4 μm as shown in Fig. 5c.

UV–visible spectroscopy study of the porphyrin micro-crystals

The electronic absorbance spectrum of meso-tetra(*N*-methy-4-pyridyl)porphyrin tetratosylate (TMPyP) in 50 mM phosphate buffer (NaPi) at room temperature exhibits an absorbance peak in the Soret region at 422 nm and four Q-bands at 519, 553, 585, and 640 nm. The electronic absorbance spectrum of zinc-tetrakis(4-sulfonatophenyl)porphyrin (Zn-TPPS) in 50 mM phosphate buffer at room temperature exhibits a Soret absorbance peak at 421 nm and two Q-bands at 556 and 597 nm as seen in Fig. 6. The locations of the absorbance peaks were determined from the second derivatives of the absorbance spectra using Grams/32. The Soret band of the porphyrin crystals formed in the presence of G4 PAMAM dendrimer

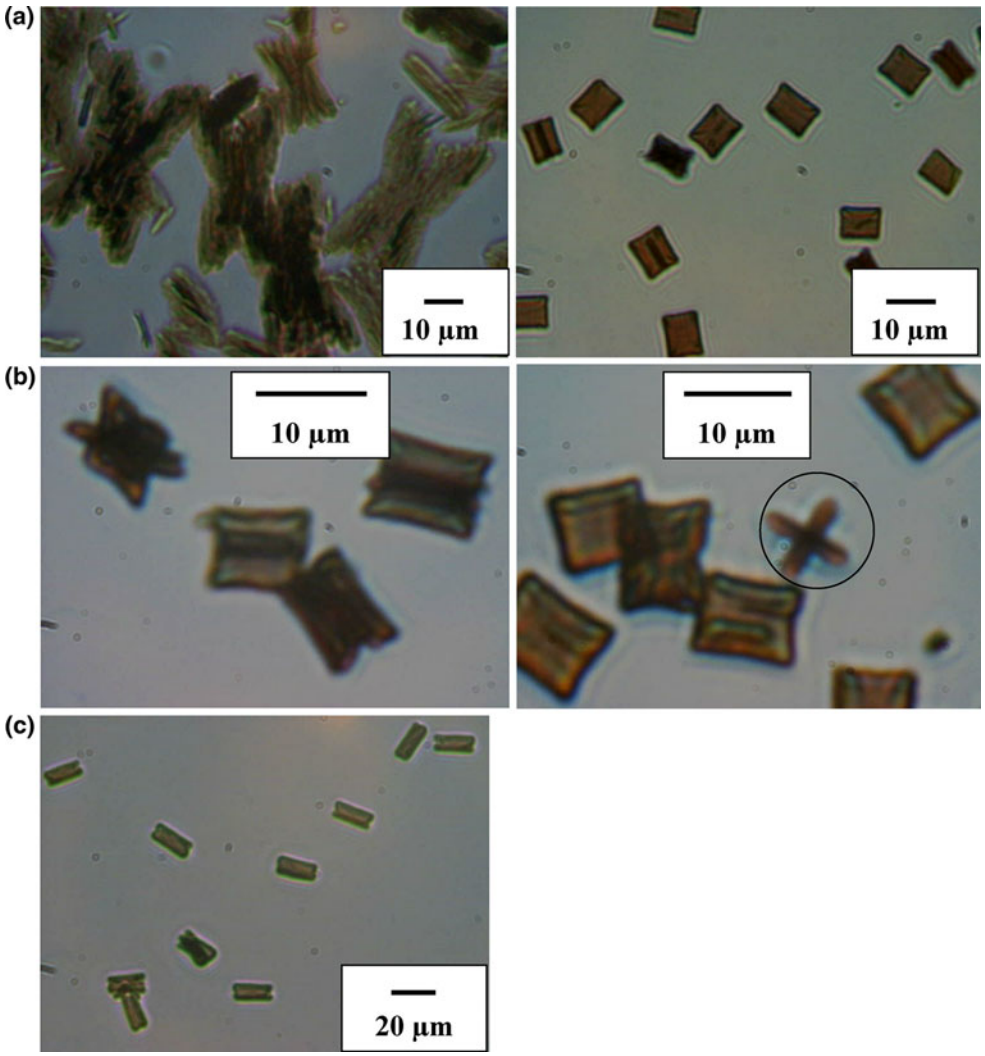

Fig. 5 Optical microscope micrograph of the porphyrin crystals formed **a** in the absence (*left*) and presence (*right*) of G4 PAMAM dendrimer with porphyrin concentration = 0.5 mM and G4 PAMAM dendrimer concentration = 1.0 mM, **b** in the presence of PAMAM dendrimer with porphyrin concentration = 0.5 mM and G4 PAMAM dendrimer concentration = 1.0 mM (while floating in solution), and **c** in the presence of G4 PAMAM dendrimer with porphyrin concentration = 0.5 mM and G4 PAMAM dendrimer concentration = 100 μM

is broadened and split into a blue-shifted band at 393 nm and a red-shifted band at 427 nm with a shoulder at 452 nm. The Q-bands of porphyrin crystals formed in the presence of G4 PAMAM dendrimer are broadened and red-shifted. The Q-bands are located at 480, 518, 566, 613, and 673 nm. The line shape of the spectrum and the locations of the absorbance peaks are independent of the crystal size and different from those of the porphyrin crystals formed in the absence of G4 PAMAM dendrimer reported in reference [7]. The locations of the absorbance peaks are not the same as those of the monomers, suggesting the complexation of the two porphyrins in the presence of the PAMAM dendrimer to form the solid porphyrin crystals instead of a mixture-aggregate of the two porphyrins.

Fluorescence spectroscopy

The fluorescence spectra of meso-tetra(*N*-methy-4-pyridyl)porphyrin (TMPyP) and zinc-tetrakis(4-sulfonatophenyl)porphyrin (Zn-TPPS) are shown in Fig. 7 along with that of the porphyrin crystals formed in the presence of G4 PAMAM dendrimer with excitation at 422, 421, and 428 nm (Soret peak absorbance wavelengths), respectively. The fluorescence spectrum of TMPyP consists of two broad and overlapping emission peaks centered at 654 nm, with a shoulder at 683 and 713 nm. The fluorescence spectrum of Zn-TPPS consists of two well-defined emission peaks at 603 and 660 nm. The fluorescence spectrum of the porphyrin crystals consists of seven well-defined emission

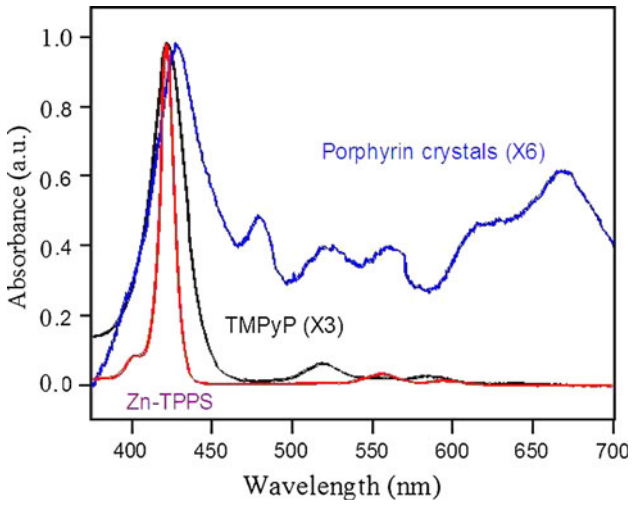

Fig. 6 Absorbance spectra of 1.6 μM meso-tetra(*N*-methy-4-pyridyl)porphyrin (TMPyP) and 1.6 μM zinc-tetrakis(4-sulfonatophenyl)porphyrin (Zn-TPPS) in 50 mM sodium phosphate (NaPi) buffer compared to the absorbance spectrum of the solid porphyrin crystals formed in the presence of G4 PAMAM dendrimer at room temperature (note the different scale)

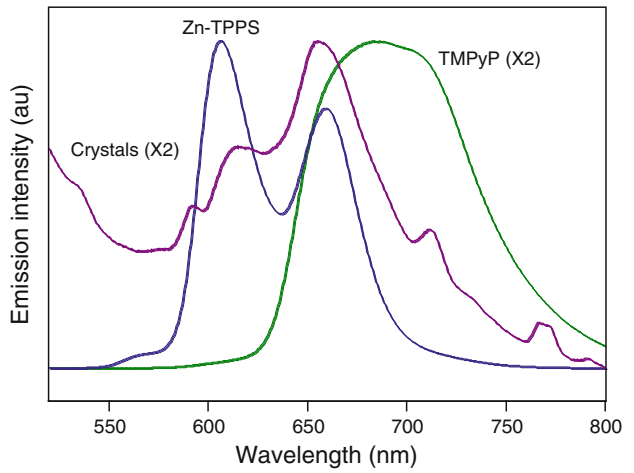

Fig. 7 Emission spectra of zinc-tetrakis(4-sulfonatophenyl)porphyrin (Zn-TPPS), meso-tetra(*N*-methyl-4-pyridyl)porphyrin (TMPyP), and the solid porphyrin crystals formed in the presence of G4 PAMAM dendrimer excited at 421, 422, and 428 nm, respectively (note the different scale)

peaks centered at 589, 611, 655 nm with a shoulder at 687, 713, 736, 770, and 790 nm.

Powder X-ray diffraction

The powder X-ray diffraction patterns of the porphyrin crystals formed in the absence and presence of G4 PAMAM dendrimer are shown in Fig. 8. The two patterns are similar with the same locations of the diffraction peaks. The relatively broadened diffraction peaks of the crystals grown in the presence of G4 PAMAM dendrimer indicate a

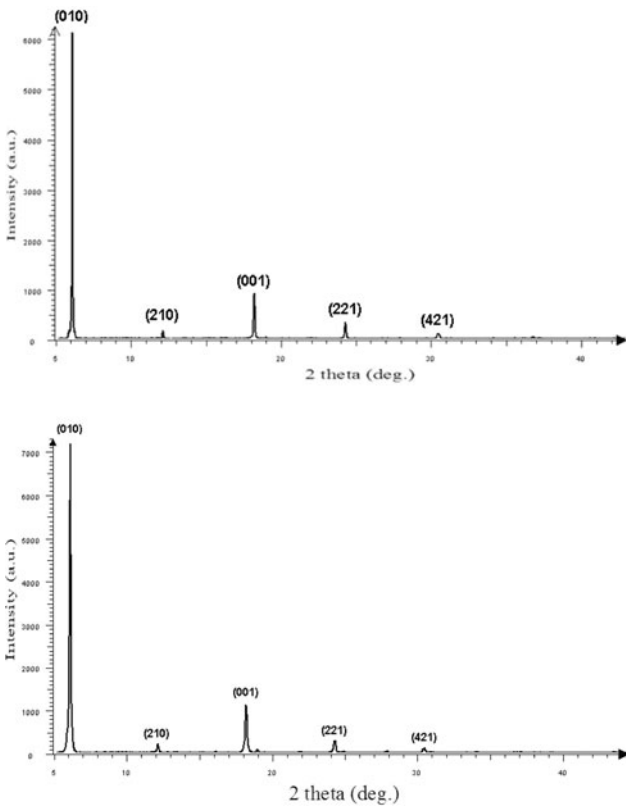

Fig. 8 Powder X-ray diffraction patterns of porphyrin crystals formed in the absence (*top*) and presence (*bottom*) of 1.0 mM G4 PAMAM dendrimer

size decrease. The porphyrin crystals formed in the presence of PAMAM dendrimer belong to the orthorhombic system with unit cell dimensions of $a = 16.94$ Å, $b = 14.58$ Å, and $c = 4.89$ Å. The volume of the unit cell is 1208.6 Å^3.

Discussion

Interaction of non-metallated cationic and anionic porphyrins with different generations of PAMAM dendrimers in aqueous solution has been reported [16]: authors have shown that porphyrins can bind to PAMAM dendrimers in aqueous solution at neutral pH resulting in a red-shift (3–8 nm, depending on the molar ratio of the porphyrin and the dendrimer in the solution) in the Soret band of the porphyrin spectrum. The anionic TPPS porphyrin can bind to the cationic PAMAM generations 2 and 4 (G2 and G4) dendrimers and form H-aggregates at pH 7.0 at high porphyrin loading as well as $H_2^{2+}TPPS^{4-}$ J-aggregates at pH 2.0 [17, 18]. The absorbance spectra in Figs. 2 and 4 strongly suggest that Zn-TPPS porphyrin is able to interact/complex with G4 PAMAM dendrimer while TMPyP is not. This is a result of the cationic nature of G4 PAMAM

dendrimer. Since the four nitrogen atoms in the core of Zn-TPPS are bound to the zinc, the complexation between the Zn-TPPS and G4 PAMAM dendrimer via binding to the pyrrole ring is unlikely to happen. Although PAMAM dendrimers are hydrophobic and potentially open to smaller hydrophobic molecules, the porphyrin molecules likely cannot enter the core of G4 PAMAM dendrimer molecules due to their comparable size (G4 PAMAM dendrimer is 46 Å and porphyrins are ~20 Å). G4 PAMAM dendrimer bears 64 positively charged amino groups. Hence, it is reasonable to assume that the positively charged amino groups (p*K*a 8.5) of the cationic G4 PAMAM dendrimer are "sites" of interaction with the negatively charged sulfonate groups of Zn-TPPS porphyrin via sulfonation reaction to form sulfonamide bonds ($R–S(=O)_2–NH–PAMAM$) as has been reported for sulfonic acid dyes and protein [19]. Ionic binding between the oppositely charged substituents on TMPyP (methylpyridinium groups with pKa about 5.0) and Zn-TPPS (sulfonate groups with pKa about 2.0) is expected between these porphyrins. We again suggest the axial coordination of Zn^{+2} ions in the core of Zn-TPPS porphyrin with two water molecules. The two water molecules bound to the zinc in Zn-TPPS porphyrin could bind axially to two unprotonated nitrogen atoms in the pyrrole rings of two TMPyP porphyrin molecules above and below the plane of the Zn-TPPS porphyrin via two hydrogen bonds as we have previously reported [15].

The red-shifts in both the Soret band and Q-bands strongly suggest the complexation of the two porphyrins in the presence of G4 PAMAM dendrimer. The locations of the absorbance peaks of the porphyrin crystals formed in the presence of G4 PAMAM dendrimer are different from those of the original porphyrin monomers. The larger blue-shift of the Soret band at 398–393 nm, the blue-shift of the Soret band at 431–427 nm, and the red-shift of the Q-bands of the porphyrin crystals formed in the presence of G4 PAMAM dendrimer with respect to the Soret band and the Q-bands of the porphyrin crystals formed in the absence of G4 PAMAM dendrimer (reported in reference [15]) suggest an unresolved influence of G4 PAMAM dendrimer on the electronic structure of the porphyrin crystals. The influence of PAMAM dendrimers on the electronic structure of multi-porphyrin supramolecular structures has not been reported. The relative red-shifts in the Q-bands and the blue-shift between the Soret spectra of porphyrin crystals formed in the presence and absence of G4 PAMAM dendrimer suggest that the addition of G4 PAMAM dendrimer to the porphyrin solution results in reducing the ionic bonding between the oppositely charged porphyrin molecules (responsible for J-aggregation) and a relative increase of the influence of other types of bonding mechanisms, such as hydrogen bonding and π–π interactions (responsible of H-aggregation), on the electronic structure of the porphyrin crystals.

The different locations of the fluorescence peaks of the porphyrin crystals further suggest the complexation of the two monomer porphyrins to form the solid crystals. The sharp well-defined fluorescence peaks suggest the immobilization of the porphyrin molecules in a solid matrix. The quenching in the porphyrin crystals fluorescence further indicates the presence of π–π interactions.

The crystal morphology can be affected/controlled by atomic interactions between the crystal surface, growth units, and additives in the starting solution. The positions of the diffraction peaks of the powder X-ray diffraction pattern of the porphyrin crystals formed in the presence of G4 PAMAM dendrimer suggests crystallization of the two porphyrins in the presence of the dendrimer to form porphyrin crystals with different size and morphology from those formed in the absence of G4 PAMAM dendrimer. The similarity between the two X-ray diffraction patterns suggests that the G4 PAMAM dendrimer is not incorporated in these porphyrin crystals but rather existed on the surface of these crystals; if the dendrimer molecules are incorporated in the porphyrin crystals, different unit cell dimensions from those of the porphyrin crystals formed in the absence of G4 PAMAM dendrimer would likely result. This indicates that the complexation between the two porphyrins is stronger than the interaction between the Zn-TPPS porphyrin and the G4 PAMAM dendrimer molecule: G4 PAMAM dendrimer molecules cannot enter the lattice sites and cannot change the crystallographic structure. The different morphology of the porphyrin crystals formed in the presence and absence of G4 PAMAM dendrimer could be explained by the fact that crystal size and morphology can be controlled under certain reaction conditions and the selection of polymers. This is in agreement with the findings that many polymers, such as poly(*N*-vinyl-2-pyrrolidone), poly-(ethylamine), PAMAM dendrimers, and poly(acrylic acid) (PAA), can effectively stabilize crystalline structures. For example:

(1) The shape of $BaWO_4$ crystals changes from whisker-like particles to right square prism when formed in the presence of PAMAM dendrimers [20].
(2) Acidic proteins and glycoproteins can interact specifically with some crystal faces, but not others inducing oriented nucleation, or can intercalate in a regular manner into the crystal lattice itself [21].
(3) In the crystallization of $CaCO_3$ in the presence of anionic PAMAM dendrimers, the dendrimer acts as a habit modifier affecting the crystal morphology upon crystallization [22].
(4) Increase in surface hardness, decrease in surface roughness, and better adhesion in Au films when

formed on a self-assembled monolayer of amine terminated polyamidoamine (PAMAM) dendrimers on SiO_x [23].

(5) Microcrystals of the organic dye, 4-*n*-octylamino-7-nitrobenz-2-oxa-1,3-diazol (NBD-C8), grown in the presence of PAMAM dendrimers have smaller size, not agglomerated, and more regular than those formed in pure water [24].

The first four examples demonstrate the control of inorganic crystal growth by dendrimers and the fifth example is the only study that supports our results on the control of organic crystal growth by G4 PAMAM dendrimer. The authors could not determine whether the dendrimer is adsorbed at the exterior or is a part of the crystal structure even with the use of different structural techniques such as elemental analysis and IR spectroscopy. However, the authors did not conduct powder X-ray diffraction study. The above examples, in addition to the strong evidence from the X-ray diffraction pattern of the porphyrin crystals, suggest the influence of G4 PAMAM dendrimer on shaping the porphyrin crystals. We speculate that the dendrimer molecules might have been adsorbed onto the surface of the porphyrin crystals and were removed in rinsing the porphyrin crystals with the pH 7.0 sodium phosphate (NaPi) buffer [25], probably resulting in altering the relative growth rates of the different crystallographic faces and leading to different crystal habits and shape.

When the G4 PAMAM dendrimer is introduced into the porphyrin solution, G4 PAMAM dendrimer interacts with Zn-TPPS as has been shown from the absorbance spectra of Zn-TPPS in the absence and presence of G4 PAMAM dendrimer (Fig. 2). In the porphyrin crystals, the crystal nucleus is Zn-TPPS and TMPyP molecules bonded via ionic bonds. Binding of G4 PAMAM dendrimer to sulfonate groups of Zn-TPPS would hinder/inhibit the ionic bonding between the porphyrin molecules. Thus, the complexation of G4 PAMAM dendrimer with Zn-TPPS porphyrin competes with the complexation of Zn-TPPS with the TMPyP porphyrin effectively blocking access to binding and growth sites at surface-located porphyrins. This would result in a larger number of crystal nuclei than would form in the absence of G4 PAMAM dendrimer: since the total content of the solute is limited and the crystal nuclei number is larger, growth of each nucleus is limited. G4 PAMAM dendrimer prevents the micro-crystals growth by binding to the negative Zn-TPPS. The smaller size of the porphyrin crystals formed in the presence of G4 PAMAM dendrimer makes these crystals a good candidate for use as a catalyst since these crystals bear higher surface area than larger crystals formed in the absence of G4 PAMAM dendrimer.

Conclusion

The formation of solid porphyrin micro-crystals using two oppositely charged water-soluble porphyrins (TMPyP and Zn-TPPS) in the presence of G4 PAMAM dendrimer was confirmed by means of optical microscopy, powder X-ray diffraction, UV–visible, and fluorescence spectroscopy. The crystals have different shapes from porphyrin crystals formed in the absence of G4 PAMAM dendrimer. The size of the crystals decreases with increasing the concentration of G4 PAMAM in the starting solution. The porphyrin crystals formed in the presence of G4 PAMAM dendrimer have different absorbance and fluorescence spectra from those of the porphyrin monomers used in making them and that of the porphyrin crystals formed in the absence of G4 PAMAM dendrimer which suggests the complexation of the two monomer porphyrins in the presence of G4 PAMAM dendrimer. The fluorescence spectrum of the crystals has well-defined fluorescence peaks and is quenched compared to those of the monomer porphyrins.

Acknowledgements This research was funded by contract no. F42620-00-D-0036 from the US Army. The cooperation and support of Dr. S.W. Kwak at the US Army Defense Ammunition Center, McAlester, OK, is appreciated.

References

1. Birks JB (1973) Organic molecular photophysics, vol 1. John Wiley, New York
2. Bargdonas S, Rotomskis R (1998) Lith J Phys 38:75
3. Kadish KM, Smith KM, Guilard R (2000) The porphyrin handbook. Academic, New York
4. Jersa M Jr, Sip M, Jersa M (1990) J Photochem Photobiol B 5:295
5. Gibbison R, Peakman TM, Maxwell JR (1995) Tetrahedron Lett 36:9057
6. Koss G, Seubert S, Seubert A, Koransky W, Kraus P, Ippen H (1980) Int J Biochem 12:1003
7. El-kholy ME, Ito O, Smith PM, D'Souza F (2004) J Photochem Photobiol C 5:79
8. Goldberg I (2005) Chem Commun 10:1243
9. Natale CD, Paolesse R, Mantini A, Macagnano A, Boschi T, D'Amico A (1998) Sens Actuators B 48:368
10. Ogawa K, Kobuke Y (2006) J Photochem Photobiol C 7:1
11. Zhou H, Groves JT (2003) Biophys Chem 105:639
12. Friedlein R, Crispin X, Osikowicz W, Braun S, De Jong MP, Simpson CD, Watson MD, Von Kieseritzky F, Samorí P, Jönsson SKM, Fahlman M, Jäckel F, Rabe JP, Hellberg J, Müllen K, Salaneck WR (2004) Synth Met 147:79
13. Lehn J, Angew M (1990) Chem Int Ed Engl 29:1304
14. Whitesides GM, Mathias JP, Seto CT (1991) Science 254:1312
15. Hikal WM, Harmon HJ (2009) Polyhedron 28:113
16. Kubat P, Lang K, Zelinger Z (2007) J Mol Liq 131:200
17. Paulo PM, Costa SM (2003) Photochem Photobiol Sci 2:597
18. Paulo PMR, Gronheid R, De Schryver FC, Costa SMB (2003) Macromolecules 36:9135
19. Tsopelas C, Sutton R (2002) J Nucl Med 43:1377

20. Zhang F, Yang SP, Chen HM, Wang ZH, Yu XB (2004) J Cryst. Growth 267:569
21. Weiner S, Addadi L (1991) Trends Biochem Sci 16(7):252
22. Naka K, Tanaka Y, Chujo Y, Ito Y (1999) Chem Commun 19:931
23. Rar A, Zhou JN, Liu WJ, Barnard JA, Bennett A, Street SC (2001) Appl Surf Sci 175:134
24. Bertorelle F, Lavabre D, Furgues F (2003) J Am Chem Soc 125(20):6244
25. Chen H, Banaszak Holl M, Orr BG, Majoros I, Klarkson BH (2003) J Dent Res 82(6):443